ISSN: 2687-8100

DOI: 10.33552/ABEB.2020.04.000589

Archives in Biomedical Engineering & Biotechnology

Iris Publishers

Review Article

Investigating the Structural and Magnetic Properties of Chitosan Coated $CoFe_2O_4$ Nanoparticles for Drug Delivery

NJ Mdlalose[1], WB Mdlalose[2]*, S.T. Dlamini[2], S. R. Mokhosi[1]

[1]*Discipline of Biochemistry, University of KwaZulu-Natal, South Africa*

[2]*Discipline of Physics, Westville Campus, University of KwaZulu-Natal, South Africa*

***Corresponding author:** Discipline of Physics, Westville Campus, University of KwaZulu-Natal, Durban 4000, South Africa.

Received Date: June 29, 2020

Published Date: July 21, 2020

Abstract

Magnetic nanoparticles (MNPs) are currently explored for use in biomedical applications, such as in MRI, hyperthermia and drug delivery. In this study, $CoFe_2O_4$ and its calcium-substituted derivative viz. CS-$Ca_{0.5}Co_{0.5}Fe_2O_4$ MNPs were synthesised via the glycol-thermal method. Furthermore, these MNPs were coated with chitosan (CS) to improve their biodegradability and biocompatibility. The anti-cancer drug, 5-fluorouracil (5-FU) was then loaded onto these MNPs to yield CS-$Ca_{0.5}Co_{0.5}Fe_2O_4$-5FU and CS-$Ca_{0.5}Co_{0.5}Fe_2O_4$-5FU. XRD results confirmed a single-phased cubic spinel structure for all MNPs. The naked MNPs displayed an average crystalline size of ~9.32 nm, which increased up to 18.20 nm upon coating. The VSM measurements recorded saturation magnetization values (Ms) of up to 73.951 emu/g. Upon polymer-coating, the shielding effect of chitosan resulted in reduced Ms of up to 17.220 emu/g in CS-$Ca_{0.5}Co_{0.5}Fe_2O_4$ MNPs. Release profiles were determined at pH 4.5 and 7.4 over a period of 72 hours. A faster release of the drug was noted at the acidic pH with an accumulative release of 91.00% in CS-CoFe2O4-5FU. Coupled with a strong recommendation for in vitro studies, these MNPs present as attractive candidates to complement current anti-cancer treatments.

Introduction

There has been a growing interest over the years in nanosized magnetic particles due to their attractive properties and potential applications within the various scientific disciplines including biomedical science [1]. When the particle size of these material decreases to below the critical diameter of 25 nm, they become superparamagnetic [2]. At room temperature, these superparamagnetic nanoparticles respond to the presence of an external magnetic field and when the field is removed, they return to a non-magnetic state [2]. For this reason, these present good feasibility for biomedical applications and have been used in targeted cancer therapy [3], hyperthermia [4] and drug delivery [5]. Although these materials provide the highest signal enhancements, they can be highly toxic to the body and are extremely sensitive to oxidation. Surface modification is thus extremely crucial before these magnetic nanoparticles (MNPs) can be considered for any biomedical applications. Commonly, iron oxide nanoparticles must be covered by an organic or inorganic biocompatible coating for a variety of reasons [6,7]. The coat will protect the MNPs from iron oxide core agglomeration, will decrease or eliminate nonspecific cell interactions and provide chemical links for the attachment of drug molecules, genetic material and targeting ligands [8].

Cobalt nanoferrrites ($CoFe_2O_4$) have in recent years gained some popularity in the science field, particularly in biomedical research due to their inherent high coercivity and anisotropy con-

stant, high saturation magnetization and ease of synthesis [6,9,10]. Various synthesis methods that have been employed have resulted in spherically shaped particles with sizes ranging between 5.6 - 28 nm which is acceptable for biomedical applications [9]. Similar to $CoFe_2O_4$ nanoferrites, $CoFe_2O_4$ MNPs have been reported to be round shaped with sizes varying within the range of 5-20nm [10]. However, their biggest downfall is due to calcium not being magnetic thus reducing the magnetization of the ferrite. Additionally, their magnetization is dependent on the synthesis method used, given that there is a wide range of methods available. These nanoferrites have been used in hyperthermia, radiotherapy on breast cancer [11] and drug delivery [12], cell labelling, cell separation, magnetically targeted carrier systems for drug delivery and in magnetic resonance imaging as contrast agents as well as for magnetofection in gene delivery [13].

Over the years, there has been increase in number and diversity of organic materials that can be used for surface coating of the MNPs to reduce their toxicity and increase their functionality. Some of these polymers include polyethylene glycol (PEG), dextran, and polyethyleneimine (PEI). Reports indicate that polymer-coating provides the MNPs with advantageous properties such as biocompatibility and increased stability in in vivo studies [8]. Chitosan (CS) is an abundant, renewable, nontoxic, and biodegradable carbohydrate polymer that is obtained from the exoskeletons of shellfish and insects. Owing to its biocompatibility, chitosan has attracted a great deal of attention as a functional biopolymer in the pharmaceutical industry [14,15,16].

Drugs such as doxorubicin, cyclophosphamide and 5-fluorouracil (5-FU) have been reported to be very powerful anti-cancer chemotherapeutic agents. 5-FU has broad spectrum of activity against solid tumours and can be employed alone or in combination with chemotherapy regimens. The mechanism behind the cytotoxicity and cell death is its interference with nucleoside metabolism in RNA and DNA [17]. By coupling polymer coated MNPs, researchers have been able to deliver these drugs to cancer cells with some successes. Challenges often relate to the chemical and physical stimulus, such as temperature, ionic strength and pH changes which can trigger the premature release of the drug before reaching the affected site [18]. A report by Sun et al., (2017) explored chitosan-coated magnetic nanoparticles as carriers for the sustained-release of 5-FU to improve the halflife of chemotherapy drugs [19].

The purpose of this research was to study the structural, magnetic and morphological properties of chitosan-functionalised $CoFe_2O_4$ and $Ca_{0.5}Co_{0.5}Fe_2O_4$. Furthermore, the coated MNPs were loaded with 5-FU and their loading efficiency and release profile evaluated.

Experimental details

MNPs synthesis

The $CoFe_2O_4$ and $Ca_{0.5}Co_{0.5}Fe_2O_4$ MNPs were produced via glycol-thermal reaction method, where stoichiometric masses of calcium chloride ($CaCI_2.6H_2O$), cobalt chloride ($Cl_2Co.2H_2O$) and iron (III) chloride ($FeCl_3.6H_2O$) hexahydrate were dissolved in about 500 ml of deionized water to produce a homogenous solution. The solution was stirred continuously for approximately 30 minutes. The precipitation of the metal chlorides was carried out by the gradual addition of 5M NaOH solution until a pH of about 9 was reached. The precipitate was then washed several times with deionized water until all the chloride ions were removed. This was confirmed by the dropwise addition of a standard solution of $AgNO_3$ to the precipitate until the water was clear and not milky. The clear water indicated that all chlorides had been removed. During the washing process, the precipitate was being filtered using Whatman glass microfibre filter (GF/F). The clean wet precursor was thereafter dispersed into 300 ml of ethylene glycol under rapid stirring. The precursor was then placed in a 500 ml glass lining in a stainless-steel pressure vessel (Watlow series model PARR 4843). The pressure vessel was then heated to 200ºC and the pressure was gradually increased to 140 psi. These conditions were held for 6 hours. The cooled products were filtered and washed with deionized water and finally with ethanol. Thereafter, the product was placed under a 200 W infrared light and was dried overnight (20 hours). The dried samples were then homogenized using an agate mortar and pestle.

Coating of magnetic nanoparticles

Chitosan coated magnetic nanoparticles were synthesized using a protocol from previous literature, with some modifications [17]. Firstly, 0.50 g of chitosan was dissolved in 100 ml of acetate buffer (pH 4.8) and stirred using the IKA RW 20 Digital Dual-Range Mixer System set at high speed (950 rpm) to produce a 0.5% chitosan solution. A pH of 4.8 was achieved by the dropwise addition of 10 M NaOH solution. Thereafter, 0.24 g of tri-polyphosphate (TPP) powder was dissolved in 100 ml of deionized water. This TPP solution was added dropwise to the chitosan solution with stirring. Finally, approximately 0.20 g of the synthesized nanoparticles (viz. $CoFe_2O_4$ and $Ca_{0.5}Co_{0.5}Fe_2O_4$) were weighed and added into the TPPchitosan mixture at a stirring speed of 450 rpm. The TPP-cross-linked CS-coated MNP mixture was left to stir for 20 hours at room temperature. Finally, the CS-$CoFe_2O_4$ and CS$Ca_{0.5}Co_{0.5}Fe_2O_4$ MNPs were separated from the black homogeneous mixture using an external magnet. After several washes with deionized water, the sample was dried under an infra-red lamp overnight. The homogenized powder was obtained using a mortar and pestle.

Drug loading

The anticancer drug 5-FU was loaded onto the chitosan coated MNPs (CS-$CoFe_2O_4$ and CS-$Ca_{0.5}Co_{0.5}Fe_2O_4$) using a method by Mushtaq et al. [6]. This was done by mixing 10 mg of CSCoFe2O4 MNPs with 25 ml of phosphate buffered saline (PBS) at pH 7.4. Thereafter, 5 mg of the drug was added to the PBS solution. The solution was placed in a shaking incubator (Infors HT Ecotron, Switzerland) set at 300 rpm at 37 °C for 48 hours. The drug-loaded MNPs (CS$CoFe_2O_4$-5FU and CS- $Ca_{0.5}Co_{0.5}Fe_2O_4$) were separated using an external magnet. They were washed a few times with deionized

water. Finally, the MNPs were dried under an infra-red lamp overnight. The incorporation of 5-FU onto the surfaces of CS- $CoFe_2O_4$ and CS- $Ca_{0.5}Co_{0.5}5Fe_2O_4$MNPs was analysed using the Jasco V-730 Bio Spectrophotometer at a wavelength of 266 nm. The absorbance readings obtained were used to calculate the drug loading capacity of the MNPs. The following equation was used to determine the loading efficiency in this equation below:

Encapsulation Efficiency (%) = (Total 5-FU added)- (free 5-FU) ×100 (Total 5-FU added)

Drug release studies

Drug release studies were conducted to assess the ability of release 5-FU over a duration of 72 hours at a physiological pH of 7.4 and acidic pH 4.5. Approximately, 1.5 mg of the coated MNP sample (CS-$CoFe_2O_4$ and CS-$CaCoFe_2O_4$) was placed and sealed in separate dialysis tubing's (MWCO = 14 000 Da). Dialysis was achieved against 5 ml of PBS at the different pHs at 37°C. At selected time intervals (0, 4, 8, 12, 16, 20, 24, 28, 32, 36, 40, 44, 48, 60 and 72 hours) a 10µl sample from each beaker was removed and analyzed using the Jasco V-730 Bio-Spectrophotometer at a wavelength of 266 nm. An equivalent amount of fresh PBS was added after each removal.

Characterizations

The X-ray diffraction (XRD) analysis was performed at room temperature to determine the phase and the average crystalline sizes of the MNPs using a Philips X-ray diffractometer monochromatic CoKα(1.788Å) radiation at ambient temperature (10–80°C) in a scale of 2θ. Functionalisation of the MNP surfaces was evaluated using the fourier transmission infra-red (FTIR) using the Perkin Elmer Spectrum 100 FTIR spectrometer. All measurements were carried out at room temperature. The morphology and microstructure of the MNPs were investigated on a high-resolution transmission electron microscope (HRTEM) using the Jeol– JEM-1010. The surface morphology of the MNPs was analyzed using the Zeiss ultra plus highresolution scanning electron microscopy (HRSEM). Stability, size distribution and the overall charge of the MNPs samples was obtained by conducting a nanoparticle tracking analysis (NTA) and zeta potential analysis using the NanoSight NS500 (Malvern Instruments,

Worcestershire, UK) at 25°C. Data was analysed using NanoSight NTA 3.2 software. Magnetic measurements of the MNPs were obtained using a LakeShore Model 735 Vibrating Sample Magnetometer, subjected to an applied magnetic field of 14 kOe at room temperature. The desired data was obtained by data acquisition software and an interface card. The VSM hysteresis loops were plotted using Origin 6.0.

Result and discussion

XRD patterns confirmed cubic spinel structure for all MNPs as presented in Figure 1. All the dominant peaks were analysed and indexed using the JCPDS Card no's (22-1086) and (770426) [6,18]. XRD analysis further showed that all NPs were single phased, and no obvious changes were noted after the coating. It has previously been reported that polymer coating do not disrupt the phases [21,6]. The full width at half maximum (FWHM) of the strongest diffraction peak (311) was used to obtain the average crystalline size (DXRD) by applying

Scherrer's formula, $DN = \beta\ k\lambda$*coscosθ [22], where K represents Scherrer's constant (0.94), λ is the wavelength of the Co–Kα X-ray source, β is the FWHM of the diffraction plane and θ is the Bragg angle. The average crystallite size of $CoFe_2O_4$ was determined to be 9.32 nm which was found to increase after coating to 13.59 nm. Also, the crystallite sizes of $Ca_{0.5}Co_{0.5}Fe_2O_4$ NPs increased from 9.33 nm to 18.20 nm post coating. These results were expected as coating and drug-loading have been reported to increase MNP sizes [7]. FTIR spectra results confirmed the presence of functional groups in all the samples as seen in (Figure 1&2).

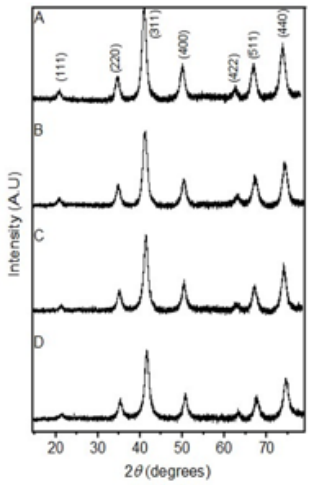

Figure 1: XRD patterns obtained for the (A)$CoFe_2O_4$ (B) CS-$CoFe_2O_4$ (C)$Ca0.5Co0.5Fe_2O_4$ and (D) CS- $Ca0.5Co0.55Fe_2O_4$ nanoparticles.

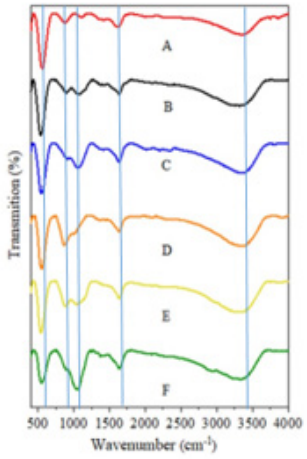

Figure 2: FTIR spectra of (A) $CoFe_2O_4$, (B) CS-$CoFe_2O_4$, (C) CS-$CoFe_2O_4$-5FU, (D) Ca0.55Co0.5Fe_2O_4, (E) CS-Ca0.5Co0.5Fe_2O_4 and (F) CS-Ca0.5Co0.5Fe_2O_4-5FU nanoparticles.

The ferrite spinel structure is featured by the absorption band around 534 cm^{-1}. Characteristically, the absorption bands are intrinsic stretching vibrations of Fe^{3+}–O^{2+} complexes at the octahedral (B) sites of the metal ions [23]. This band is present in all the FTIR spectra of the NPs. Hence, this confirmed that the synthesised, coated and loaded samples possessed a spinel structure. The presence of this peak even after coating and drug loading suggests that the structure remains intact and is not destabilised by chitosan or the drug. Another broad peak at 3454 cm^{-1} which is assigned to O-H stretching vibrations was observed on all samples representing absorbed or free water on their surfaces [23,24]. The peaks around 1634cm−1 were observed to be much more intense for the chitosan-coated derivatives, i.e. CS- $CoFe_2O_4$, CS-$CoFe_2O_4$-5FU, CS-$Ca_{0.5}Co_{0.5}Fe_2O_4$ and CS- $Ca_{0.5}Co_{0.5}5Fe_2O_4$-5FU MNPs. This is attributed to the characteristic N-H bending due to amide groups of chitosan. The peak observed at 1019 cm^{-1}, an additional intense peak is observed characteristic of the C-O-C stretching vibrations specifically in the drug-loaded MNPs. This suggests that the drug was loaded successfully, and the shift suggests successful encapsulation of the drug [25]. An interesting peak is represented in the region of 900 cm-1 and is linked to the metal oxide vibrations i.e. Co-Fe and Ca-Fe [7].

Morphological differences were noted between the derivatives with the cobalt ferrites NPs presenting near-perfect spheres (Figure 5). The calcium ferrite NPs, viz $Ca_{0.5}Co_{0.5}5Fe_2O_4$, CS$Ca_{0.5}Co_{0.5}5Fe_2O_4$ and CS-$Ca_{0.5}Co_{0.5}Fe_2O_4$-5FU were more quasi-spherical in shape. The drugloaded NPs had a thick coating around the core-shell and it appeared that the MNPs agglomerated even further after inclusion of the drug. Interestingly, the average diameters (DHRTEM) determined from the particle size distributions showed an increase in particle size of up to 11 and 13 nm for the CS-$CoFe_2O_4$-5FU and CS-$Ca_{0.5}Co_{0.5}Fe_2O_4$-5FU, respectively (Figure 4) as expected (Figure 3&4).

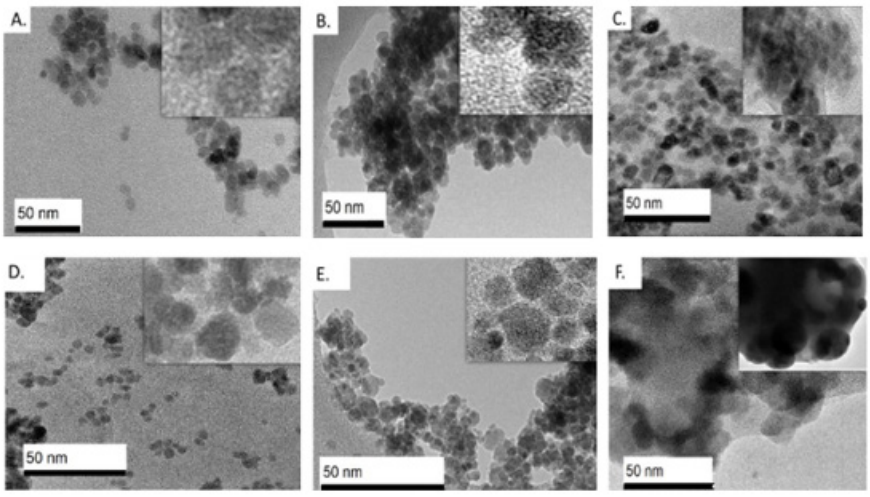

Figure 3: HRTEM images for (A) $CoFe_2O_4$, (B) CS-$CoFe_2O_4$, (C) CS-$CoFe_2O_4$-5FU, (D) Ca0.5Co0.5Fe_2O_4, (E) CS- Ca0.5Co0.5$Fe_2O_4$and (F) CS- Ca0.5Co0.5Fe_2O_4-5FU nanoparticles.

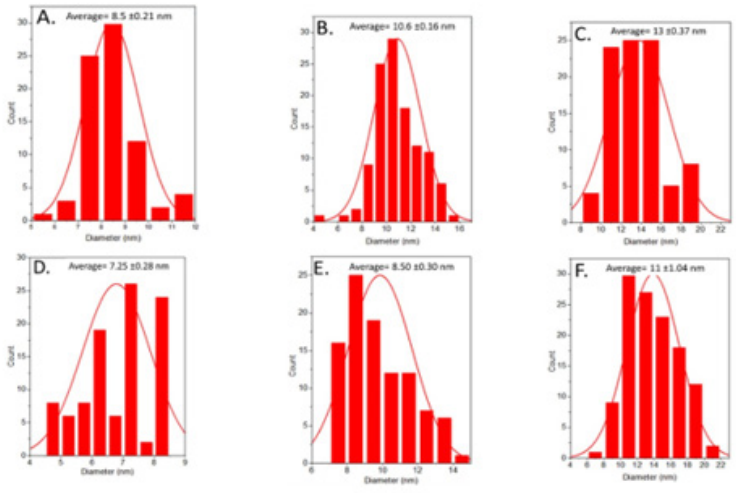

Figure 4: Particle size distributions for (A) $CoFe_2O_4$, (B) CS-$CoFe_2O_4$, (C) CS-$CoFe_2O_4$-5FU, (D) $Ca0.5Co0.5Fe_2O_4$, (E) CS-$Ca0.5Co0.5Fe_2O_4$ and (F) CS-$Ca0.5Co0.5Fe_2O_4$-5FU NPs.

HRTEM, XRD and NTA size measurements showed no significant size differences between the naked cobalt and calcium cobalt ferrite NPs as listed in Table 1. An increase was however, observed with chitosan-functionalisation where CS-$Ca_{0.5}Co_{0.5}Fe_2O_4$ hydrodynamic size diameters measured up to 130 nm. The hydrodynamic sizes (DH) from the NTA were expectedly larger as was reported in previous studies [30]. This is because the measurements are based on the scattering of light in a colloidal suspension, and additionally often the aggregated particles are considered to be single particles [26]. At sizes below 200 nm, these MNPs can be proficiently used as drug delivery systems [27].

Table 1: XRD, HRTEM and NTA size and zeta potential measurements for the nanoparticles.

	DHRTEM (nm)	DXRD (nm)	DH (nm)	ζ-potential (mV)
	± 0.39	± 4.67	± 9.15	± 3.03
$CoFe_2O_4$	8.5	9.32	103.5	15.1
CS-$CoFe_2O_4$	10.6	13.59	120	20.5
CS-$CoFe_2O_4$-5FU	13	-	-	-
$Ca_{0.5}Co_{0.5}Fe_2O_4$	7.25	9.33	105	12.3
CS-$Ca_{0.5}Co_{0.5}Fe_2O_4$	8.25	18.2	130	25
CS-$Ca_{0.5}Co_{0.5}Fe_2O_4$-5FU	11.4	-	-	-

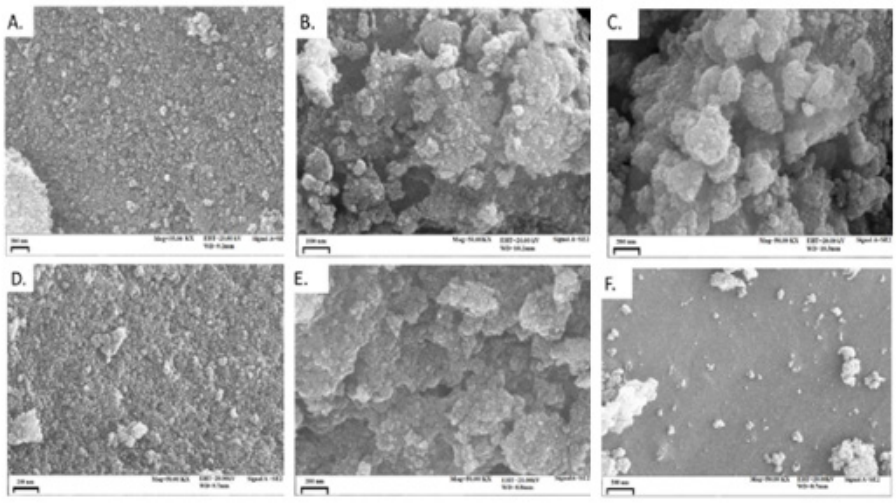

Figure 5: HRSEM images of (A) $CoFe_2O_4$, (B) CS-$CoFe_2O_4$, (C) CS-$CoFe_2O_4$-5FU, (D) $Ca0.5Co0.5Fe_2O_4$, (E) CS-$Ca0.5Co0.5Fe_2O_4$ and (F) CS-$Ca0.5Co0.5Fe_2O_4$-5FU nanoparticles.

Surface charges of the MNPs were analysed using the zeta potential measurements. The observed zeta potentials for $CoFe_2O_4$, CS-$CoFe_2O_4$, $Ca_{0.5}Co_{0.5}Fe_2O_4$ and CS- $Ca_{0.5}Co_{0.5}Fe_2O_4$ MNPs are 15.1 mV, 20.5 mV, 12.3 mV and 25.0 mV, respectively. The positive zeta potential measurement obtained could have occurred due to the overall charge of the MNPs being +2 which resulted in the particles forming a steady suspension in water [28]. There was an increase in zeta potential measurements which suggested that coating enhanced stability of the NPs [28]. HRSEM images indicated overall spherical and agglomerated MNPs as observed in Figure 5. This is indicative of higher interactions between the particles when in suspension (Figure 5).

EDX results confirmed quantified elemental compositions of the synthesised NPs as presented in Figure 4. In all of the samples, there was a notable prevalence of Fe, Co and O peaks detected. An additional Ca peak was observed for the $Ca_{0.5}Co_{0.5}Fe_2O_4$ sample which confirmed successful substitution of calcium. The chitosan coated derivatives all presented with new elements in their composition. Most importantly, nitrogen (N) was attributed to chitosan functionalization onto the MNP surfaces [29]. This resulted in slight % weight decrease of Fe and O in the MNP. The presence of phosphorus (P) and sodium (Na) were probably derived from the synthesis components from not having been washed off thoroughly while the silica contaminant could be particulates from the glassware used. The peaks of gold (Au) were also detected on all the spectrums since it was used as a sample coating agent. Chlorine was detected only in the drug-loaded CS- $Ca_{0.5}Co_{0.5}Fe_2O_4$-5FU and CS- $Ca_{0.5}Co_{0.5}Fe_2O_4$-5FU was observed in the micrographs of the drug loaded samples which confirmed the presence of the anti-cancer drug. The presence of the anti-cancer drug resulted to an increase in the agglomeration (see Figure 3 (C) and (F)). Hence, the anti-cancer drug was successfully loaded on the coated samples (Figure 6).

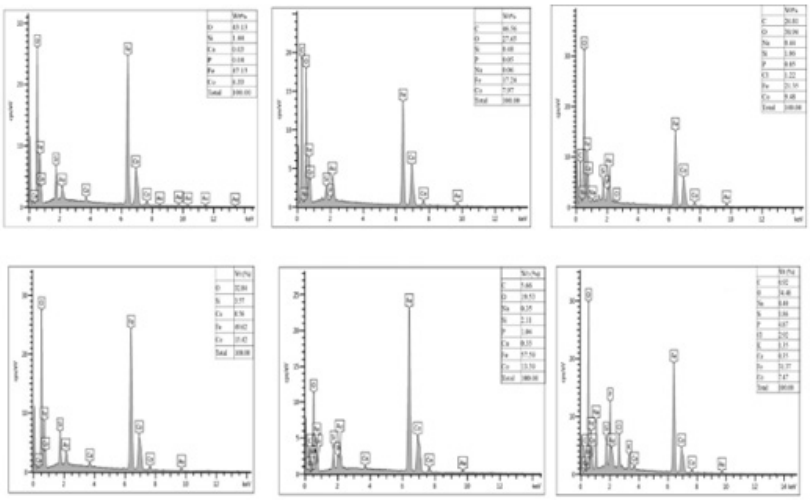

Figure 6: EDX micrographs for (A) $CoFe_2O_4$, (B) CS-$CoFe_2O_4$, (C) CS-$CoFe_2O_4$-5FU, (D) Ca0.5Co0.5Fe_2O_4, (E) CS- Ca0.5Co0.5Fe_2O_4 and (F) CS- Ca0.5Co0.5Fe_2O_4-5FU nanoparticles

The hysteresis loops and saturation magnetization (MS) were obtained under magnetic fields of up to 14kOe at room temperature (Figure 7 and Table 2). All samples exhibited "S" shape hysteresis loops and all NPs were superparamagnetic in nature [2] (Figure 7).

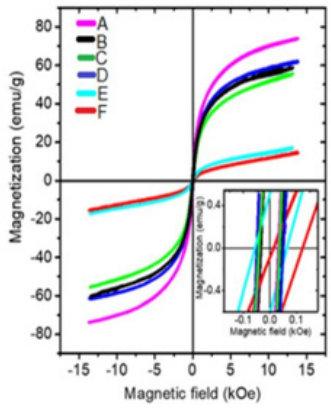

Figure 7: Hysteresis loops of (A) $CoFe_2O_4$, (B) CS-$CoFe_2O_4$, (C) CS-$CoFe_2O_4$-5FU, (D) Ca0.5Co0.5Fe_2O_4, (E) CS-Ca0.5Co0.5Fe_2O_4 and (F) CS- Ca0.5Co0.5Fe_2O_4 -5FU nanoparticles.

Table 2: Saturation magnetization (MS) and coercivity (HC) measurements for the MNPs.

	MS (emu/g) ± 0.005	HC (Oe) ± 0.005
$CoFe_2O_4$	73.951	31.949
CS-$CoFe_2O_4$	59.633	38.954
CS-$CoFe_2O_4$-5FU	55.55	36.654
$Ca_{0.5}Co_{0.5}Fe_2O_4$	61.833	51.294
CS- $Ca_{0.5}5Co_{0.5}Fe_2O_4$	17.22	60.594
CS-$Ca_{0.5}Co_{0.5}Fe_2O_4$-5FU	15.189	55.48

$Ca_{0.5}Co_{0.5}Fe_2O_4$ NPs presented with slightly lower saturation magnetization compared to $CoFe_2O_4$ NPs. This can be explained by the weakening of exchange interactions with the inclusion of the non-magnetic Ca^{2+} ions [2]. Both $CoFe_2O_4$ and $Ca_{0.5}Co_{0.5}Fe_2O_4$ NPs decreased with coating from 73.866 to 59.633 emu/g and 61.833 to 17.220 emu/g, respectively. This reduction is attributed to the shielding effect induced by the chitosan layer around the surface of the MNPs [7]. The drastic reduction observed with the $Ca_{0.5}Co_{0.5}Fe_2O_4$ NPs after coating could be a result of a transformation from the multi-domain to a single domain structure for the NPs [2].

Loading of the 5-FU resulted in further but marginal decrease in the MS values. This was expected as the drug possesses non-magnetic ions, as reported by Anirudha et al. (2015) [30]. A slight increment of the coercive field (HC) was observed for both $CoFe_2O_4$ and $Ca_{0.5}Co_{0.5}Fe_2O_4$ samples after coating. Coercivity values tend to be lower for polymer-coated NPs as the polymer may interfere with the NP domain walls. This necessitates for an increased magnetic field that must be applied to close the loop [7,34].

Drug encapsulation efficiencies for CS-$CoFe_2O_4$-5FU and CS- $Ca_{0.5}Co_{0.5}Fe_2O_4$-5FU were found to be 92.77% and 81.68%, respectively. CS-$CoFe_2O_4$ displayed superior interactions between the positively charged chitosan on the surface of $CoFe_2O_4$ and the negatively charged drug and hence the better encapsulation [18]. Figure 8 shows drug release profile of how readily the drug was released from the MNPs at pH 4.5 (solid lines) and pH 7.4 (dotted lines) over 72 hours [6].

Figure 8: Release profile studies of 5-FU from MNPs. CS-$CoFe_2O_4$-5FU NPs are represented in red (A and C) and CS- $Ca_{0.5}Co_{0.5}Fe_2O_4$-5FU NPs are represented in black (B and D). The solid line corresponds with pH 4.5, while the dotted lines correspond with pH 7.4.

Approximately 91% of the drug was released after 36 hours at the acidic tumour microenvironment from the CS-$CoFe_2O_4$-5FU NPs. This was more than the 74% release by the calcium-substituted cobalt NPs. The faster drug release from CS-$CoFe_2O_4$-5FU indicated that the majority of the drug was encapsulated closer to the surface of the MNPs and that the MNPs had a larger surface area to volume ratio [32]. A similar trend was observed at pH 7.4 where the accumulative release percentages were found to be 96.97% and 85% after 60 hours of release. This pH-dependent release was reported previously by Balasubramanian [33]. Overall, the release of 5-FU was sustained and increased gradually in a linear trend until an optimum was reached. No sudden diffusion or bust release of the drug from the MNPs, which is an important factor in drug delivery. This often means that the drug may be released prematurely before reaching the target site [34]. Factors that may impact on drug release rate from MNPs include the intensity of the hydrophilic interactions, the degree of cross linking between the chitosan and 5-FU, the swelling of the MNPs in aqueous medium and the degradation of the polymer layer in aqueous medium [35]. This indicated that both MNP derivatives present for sufficient release of 5-FU released under acidic condition, suggesting that their application may result in the majority of the drug accumulating on cancerous cells [18].

Conclusion

In this study, $CoFe_2O_4$ and $Ca_{0.5}Co_{0.5}Fe_2O_4$were synthesized successfully via the glycolthermal method, they were functionalised with the polymer chitosan and loaded with the drug 5-FU. The MNPs possessed sufficient magnetic properties for biomedical application with $CoFe_2O_4$ derivatives exhibiting the highest saturation magnetisation. Additionally, the coated cobalt ferrite presented with excellent drug encapsulation efficiency and a faster release profile compared to the $Ca_{0.5}Co_{0.5}Fe_2O_4$. Most significantly, both MNPs displayed pH-dependent release with an enhanced release profile at the tumour micro-environment with acidic pH than at physiological pH 7. With a strong recommendation for further in vitro studies, above findings provide a strong basis for both chitosan coated $CoFe_2O_4$ and $Ca_{0.5}Co_{0.5}Fe_2O_4$ MNPs to be considered as feasible drug delivery vehicles in cancer treatment.

Acknowledgement

None.

Conflicts of Interest

No conflicts of interest.

References

1. PM Price, WE Mahmoud, AA Al-Ghamdi, LM Bronstein (2018) Magnetic drug delivery: Where the field is going. Frontiers in Chemistry 6: 619.
2. M Houshiar, F Zebhi, ZJ Razi, A Alidoust, Z Askari (2014) Synthesis of cobalt ferrite ($CoFe_2O_4$) nanoparticles using combustion, coprecipitation, and precipitation methods: A comparison study of size, structural, and magnetic properties. Journal of Magnetism and Magnetic Materials 371: 43-48.

3. K Tajiri, K Aonuma, I Sekine Cardiovascular toxic effects of targeted cancer therapy. Japanese Journal of Clinical Oncology 47(9): 779-785.

4. VD Kassabova-Zhetcheva, LP Pavlova, BI Samuneva, ZP Cherkezova-Zheleva, IG Mitov, et al. (2007) Characterization of superparamagnetic MgxZn1-x Fe_2O_4 powders. Central European Journal of Chemistry 5(1): 107-117.

5. C Binns (2014) Medical applications of magnetic nanoparticles. Frontiers in Nanoscience and Nanotechnology 6(1): 217-258.

6. MW Mushtaq, F Kanwal, A Batool, T Jamil, M Zia-ul-Haq, et al. (2017) Polymer-coated $CoFe_2O_4$ nanoassemblies as biocompatible magnetic nanocarriers for anticancer drug delivery. Journal of Materials Science 52(16): 9282-9293.

7. WB Mdlalose, SR Mokhosi, S Dlamini, T Moyo, M Singh Effect of chitosan coating on the structural and magnetic properties of $MnFe_2O_4$ and $Mn_{0.5}Co_{0.5}Fe_2O_4$ nanoparticles. AIP Advances 8(5): 0-6.

8. Z Hedayatnasab, F Abnisa, WMAW Daud (2017) Review on magnetic nanoparticles for magnetic nanofluid hyperthermia application. Materials and Design 123(1): 174-196.

9. CR Stein, MTS Bezerra, GHA Holanda, J Andre-Filho, PC Morais (2018) Structural and magnetic properties of cobalt ferrite nanoparticles synthesized by co-precipitation at increasing temperatures. AIP Advances 8: 5.

10. Y Jumril, S Noor Humam, G Mariyam Jameelah (2018) Synthesis of calcium ferrite nanoparticles ($CaFe_2O_4$-NPs) using auto-combustion method for targeted drug delivery, Key Engineering Materials. Trans Tech Publications Ltd 775: 115-119.

11. V Verma, C Shah, MP Mehta (2016) Clinical Outcomes and Toxicity of Proton Radiotherapy for Breast Cancer. Clinical Breast Cancer 16(3): 145-154.

12. G Wang, Y Ma, Z Wei, M Qi (2016) Development of multifunctional cobalt ferrite/graphene oxide nanocomposites for magnetic resonance imaging and controlled drug delivery. Chemical Engineering Journal 289(1): 150-160.

13. K Syal, M Mo, H Yu, R Iriya, W Jing, et al. (2017) Current and emerging techniques for antibiotic susceptibility tests. Theranostics 7(7): 1795-1805.

14. O Arum, RK Boparai, JK Saleh, F Wang, AL Dirks, et al. (2014) Specific suppression of insulin sensitivity in growth hormone receptor gene-disrupted (GHR-KO) mice attenuates phenotypic features of slow aging. Aging Cell 13(6): 981-1000.

15. M Ziegler Borowska, D Chełminiak, H Kaczmarek (2015) Thermal stability of magnetic nanoparticles coated by blends of modified chitosan and poly(quaternary ammonium) salt. Journal of Thermal Analysis and Calorimetry 119: 499–506.

16. V Raj, G Prabha (2016) Synthesis, characterization and in vitro drug release of cisplatin loaded Cassava starch acetate–PEG/gelatin nanocomposites. Journal of the Association of Arab Universities for Basic and Applied Sciences 21: 10-16.

17. KS Tummala, AL Gomes, M Yilmaz, O Grana, L Bakiri, et al. (2014) Inhibition of De Novo NAD+ Synthesis by Oncogenic URI Causes Liver Tumorigenesis through DNA Damage. Cancer Cell 26: 826-839.

18. RS Tigli Aydin, M Pulat (2012) 5-fluorouracil encapsulated chitosan nanoparticles for pHstimulated drug delivery: Evaluation of controlled release kinetics. Journal of Nanomaterials 2012: 42.

19. Y Sun, X Zuo, SKRS Sankaranarayanan, S Peng, B Narayanan, et al. (2017) Quantitative 3D evolution of colloidal nanoparticle oxidation in solution. Science 80(356): 303–307.

20. V Corral-Flores, D Bueno-Baques, RF Ziolo (2010) Synthesis and characterization of novel $CoFe_2O_4$-$BaTiO_3$ multiferroic core-shell-type nanostructures. Acta Materialia 58(3): 764-769.

21. N Asadi, N Annabi, E Mostafavi, M Anzabi, R Khalilov, et al. (2018) Synthesis, characterization and in vitro evaluation of magnetic nanoparticles modified with PCL–PEG–PCL for controlled delivery of 5FU. Artificial Cells, Blood Substitutes, and Biotechnology 46: 938-945.

22. K Venkatesan, D Rajan Babu, MP Kavya Bai, R Supriya, R Vidya, et al. (2015) Structural and magnetic properties of cobaltdoped iron oxide nanoparticles prepared by solution combustion method for biomedical applications. International Journal of Nanomedicine 10: 189-198.

23. G Unsoy, S Yalcin, R Khodadust, P Mutlu (2012) In situ synthesis and characterization of chitosan coated iron oxide nanoparticles and loading of doxorubicin. nano con 23: 10.

24. RL Siegel, KD Miller, A Jemal, KI Alcaraz (2016) Cancer statistics. Cancer Journal for Clinicians 66: 7-30.

25. D Kaushik, S Sardana, D Mishra (2010) In vitro characterization and cytotoxicity analysis of 5-Fluorouracil loaded chitosan microspheres for targeting colon cancer. Indian Journal of Pharmaceutical Education and Research 44(3): 274-282.

26. CM Cirtiu, T Raychoudhury, S Ghoshal (2011) A Moores Systematic comparison of the size, surface characteristics and colloidal stability of zero valent iron nanoparticles pre-and post-grafted with common polymers. Colloids and Surfaces A: Physicochemical and Engineering Aspects 390(1-3): 95-104.

27. L De Marchi, F Coppola, AMVM Soares, C Pretti, JM Monserrat, et al. (2019) Engineered nanomaterials: From their properties and applications, to their toxicity towards marine bivalves in a changing environment, Environmental Research 178: 108683.

28. O Salata (2004) Applications of nanoparticles in biology and medicine, Journal of Nanobiotechnology 3.

29. Y Ding, SZ Shen, H Sun, K Sun, F Liu, et al. (2015) Design and construction of polymerized-chitosan coated Fe_3O_4 magnetic nanoparticles and its application for hydrophobic drug delivery. Materials Science and Engineering C 48: 487-498.

30. D Kaushik, S Sardana, D Mishra (2010) In vitro characterization and cytotoxicity analysis of 5-Fluorouracil loaded chitosan microspheres for targeting colon cancer. Indian Journal of Pharmaceutical Education and Research 44(3): 274-282.

31. A Samariya, SN Dolia, AS Prasad, PK Sharma, SP Pareek, et al. (2013) Size dependent structural and magnetic behaviour of $CaFe_2O_4$. Applied Surface Science p 830-835.

32. P Singh, S Pandit, VRSS Mokkapati, A Garg, V Ravikumar, et al. (2018) Gold nanoparticles in diagnostics and therapeutics for human cancer. International Journal of Molecular Sciences 19: 1.

33. S Balasubramanian, A Ravindran Girija, Y Nagaoka, S Iwai, M Suzuki, et al. (2014) Curcumin and 5-Fluorouracilloaded, folate- and transferrin-decorated polymeric magnetic nanoformulation: A synergistic cancer therapeutic approach. accelerated by magnetic hyperthermia, International Journal of Nanomedicine 9(1): 437-459.

34. S Sadighian, K Rostamizadeh, H Hosseini-Monfared, M Hamidi (2014) Doxorubicinconjugated core-shell magnetite nanoparticles as dual-targeting carriers for anticancer drug delivery. Colloids and Surfaces B: Biointerfaces 117: 406.

35. V Balan, G Dodi, N Tudorachi, O Ponta, V Simon, et al. (2015) Doxorubicin-loaded magnetic nanocapsules based on N-palmitoyl chitosan and magnetite: Synthesis and characterization. Chemical Engineering Journal 279:1.